

**ARTICLE**

# HIV-1-induced type I IFNs promote viral latency in macrophages

Laura L. Dickey | Laura J. Martins | Vicente Planelles | Timothy M. Hanley

Department of Pathology, University of Utah  
School of Medicine, Salt Lake City, Utah, USA**Correspondence**Timothy M. Hanley, Department of Pathology,  
University of Utah School of Medicine, 15N  
Medical Drive East, Salt Lake City, UT 84112,  
USA.Email: [timothy.hanley@hsc.utah.edu](mailto:timothy.hanley@hsc.utah.edu)Additional supporting information can be  
found online in the Supporting Information  
section at the end of this article.**Abstract**

Macrophages chronically infected with HIV-1 serve as a reservoir that contributes to HIV-1 persistence during antiretroviral therapy; however, the mechanisms governing the establishment and maintenance of this virus reservoir have not been fully elucidated. Here, we show that HIV-1 enters a state reminiscent of latency in monocyte-derived macrophages (MDMs), characterized by integrated proviral DNA with decreased viral transcription. This quiescent state is associated with decreased NF- $\kappa$ B p65, RNA polymerase II, and p-TEFb recruitment to the HIV-1 promoter as well as maintenance of promoter chromatin in a transcriptionally nonpermissive state. MDM transition to viral latency is mediated by type I IFN signaling, as inhibiting type I IFN signaling or blocking type 1 IFN prevents the establishment of latent infection. Knockdown studies demonstrate that the innate immune signaling molecule mitochondrial antiviral signaling protein (MAVS) is required for the transition to latency. Finally, we demonstrate a role for the viral accessory protein Vpr in the establishment of HIV-1 latency in macrophages. Our data indicate that HIV-1-induced type I IFN production is responsible for the establishment of viral latency in MDMs and identify possible therapeutic targets for the prevention or elimination of this important HIV-1 reservoir.

**KEYWORDS**HIV-1, IFN, latency, macrophage, MAVS, NF- $\kappa$ B**1 | INTRODUCTION**

With the advent of antiretroviral therapy (ART), HIV-1 infection has become a chronic disease in industrialized countries. Unfortunately, there is no cure for HIV-1 and infected individuals require lifelong ART and are at increased risk for multiple comorbidities, including cardiovascular, metabolic, and neurologic disease.<sup>1</sup> The major barrier to the eradication of HIV-1 infection is the presence of small reservoirs of latently or persistently infected cells that escape immune-mediated clearance and the effects of therapy. These include CD4+ T cells<sup>2-6</sup> and

possibly macrophages.<sup>7</sup> There remain crucial gaps in our understanding of the molecular mechanisms that lead to transcriptionally silent or latent HIV-1 infection in macrophages. Because a functional cure for HIV-1 will require the elimination of both T-cell and myeloid reservoirs, it is imperative that we understand the mechanisms that underlie the establishment and maintenance of viral latency or persistence in macrophages.

Whether HIV-1 replicates constitutively or establishes a true latent state in macrophages remains unclear despite over three decades of research. HIV-1-infected macrophages have been detected in many

This is an open access article under the terms of the [Creative Commons Attribution-NonCommercial](https://creativecommons.org/licenses/by-nc/4.0/) License, which permits use, distribution and reproduction in any medium, provided the original work is properly cited and is not used for commercial purposes.

© 2022 The Authors. *Journal of Leukocyte Biology* published by Wiley Periodicals LLC on behalf of Society for Leukocyte Biology.

tissues in the body, including the CNS, lymph nodes, lungs, liver, kidneys, and gastrointestinal system, and are thought to contribute to inflammation and tissue damage despite immune reconstitution achieved by ART-induced viral suppression.<sup>8,9</sup> Recent studies in humans and animal models have shown that myeloid cells can serve as a durable reservoir in the setting of ongoing ART.<sup>10–16</sup> These studies demonstrate that myeloid cells represent a clinically important viral reservoir that, together with the T-cell reservoir, must be addressed if viral eradication is to be achieved.

Previous work from our group and others demonstrated that macrophages may serve as reservoirs for latent HIV-1. For example, M1-polarized monocyte-derived macrophages (MDMs) infected with HIV-1 and then restimulated with either IFN- $\gamma$  or TNF- $\alpha$  demonstrate near undetectable levels of viral transcripts, but are inducible in a manner consistent with latent infection.<sup>11</sup> In addition, sorted HIV-1-infected MDMs without detectable virus expression can undergo spontaneous, low-level viral reactivation and can also be reactivated by latency reversing agents (LRAs).<sup>16</sup> These *in vitro* macrophage models of HIV-1 latency are complemented by findings using *ex vivo* macrophages from SIV-infected macaques, which have been shown to harbor SIV genomes that can be reactivated by LRAs to produce infectious virus.<sup>14</sup> Our previous studies demonstrated that HIV-1 infection of macrophages is highly immunogenic and is capable of inducing dramatic changes in cellular gene expression that are consistent with suboptimal type I, type II, and type III IFN responses,<sup>17</sup> in that the IFN response is muted compared to treatment with exogenous IFNs.<sup>18</sup> Furthermore, we have shown that coinfection with bacteria that induce a type I IFN response creates a state reminiscent of viral latency in HIV-1-infected macrophages.<sup>15</sup> Based on these findings, we hypothesized that HIV-induced type I IFN production promotes viral persistence through the establishment of latent infection in macrophages.

Here, we use an *in vitro* MDM model to delineate factors involved in establishing latent HIV-1 infection in macrophages. Our data identify a central role for type I IFN signaling in this process. Type I IFN signaling is associated with changes in the recruitment of transcription factors to the viral promoter during the course of infection as HIV-1 enters latency, and the transition to latency in HIV-1-infected MDMs requires MAVS signaling. Finally, we demonstrate that the viral accessory protein Vpr induces a muted type I IFN response that contributes to the establishment of viral latency in MDMs. These studies enhance our understanding of viral latency and persistence in macrophages and highlight potential avenues for the development of therapeutics targeting this important reservoir.

## 2 | MATERIALS AND METHODS

### 2.1 | Ethics statement

This research has been determined to be exempt by the Institutional Review Board of University of Utah Health since it does not meet the definition of human subjects research.

### 2.2 | Isolation and culture of primary cells

Human PBMCs were isolated from leukoreduction filters (Haemonetics) obtained from healthy donors by density gradient centrifugation. Primary CD14<sup>+</sup> monocytes were isolated from PBMCs using mouse anti-human CD14 monoclonal antibody-conjugated magnetic beads and LS MACS cell separation columns (Miltenyi Biotec) according to the manufacturer's protocol. Primary MDMs were generated by culturing CD14<sup>+</sup> monocytes in RPMI-1640 with 10% human AB serum, 10% FBS, 100 U/ml penicillin (Gibco), 100  $\mu$ g/ml streptomycin (Gibco), and 0.29 mg/ml L-glutamine (Gibco) for 6 days to differentiate into MDMs. Following differentiation, MDMs were cultured in RPMI-1640 supplemented with 10% FBS, 100 U/ml penicillin, 100  $\mu$ g/ml streptomycin, and 0.29 mg/ml L-glutamine. The genetic sex of a subset of the donors was determined by PCR amplification of the SRY gene located on the Y chromosome. PM1 cells were cultured in RPMI-1640 supplemented with 10% FBS, 100 U/ml penicillin, 100  $\mu$ g/ml streptomycin, and 0.29 mg/ml L-glutamine. 293T cells were cultured in DMEM supplemented with 10% FBS, 100 U/ml penicillin, 100  $\mu$ g/ml streptomycin, and 0.29 mg/ml L-glutamine.

### 2.3 | IFNs, biologics, and chemical inhibitors

PAM3CSK4 was purchased from Invivogen and was reconstituted in endotoxin-free H<sub>2</sub>O. IFN- $\alpha$  and IFN- $\beta$  were purchased from PBL Interferon Source. B18R was purchased from R&D Systems. TNF- $\alpha$  was purchased from PeproTech. PMA (Sigma), TLR3 inhibitor (Calbiochem), TLR7/8 inhibitor ODN20959 (Miltenyi), A151 (Invivogen), ruxolitinib (MedChemExpress), itacitinib (MedChemExpress), bafilomycin (Invivogen), BX795 (Invivogen), MRT67037 (Invivogen), H-151 (Invivogen), G150 (Selleckchem), and RU.521 (Invivogen) were reconstituted in DMSO or sterile deionized water.

### 2.4 | Virus production

Replication-competent HIV-1<sub>BaL</sub> was generated by infection of PM1 cells as described previously.<sup>19</sup> Single-round replication-competent HIV-1 reporter viruses were generated by packaging a nanoluciferase expressing reporter virus, DHIV3-nanoluciferase, an enhanced green fluorescent protein expressing reporter virus, DHIV3-GFP, or an mCherry expressing reporter virus, DHIV3-mCherry, with the envelope glycoproteins from vesicular stomatitis virus (VSV; VSV-G) or amphotropic murine leukemia virus (A-MLV). In these constructs, reporter gene expression is under the control of the 5' LTR. Reporter virus stocks were generated by transfecting HEK293T cells using the calcium phosphate method as described previously.<sup>19</sup> Replication competent HIV-1<sub>BaL</sub> encoding murine CD24 was generated by transfecting 293FT cells with pNL4-3-BaL-IRES-HSA using the calcium phosphate method. Cell supernatants were harvested 48 h posttransfection, filtered through a 0.45  $\mu$ m filter, and stored at  $-80^{\circ}\text{C}$  until use. p24<sup>gag</sup> content was determined by ELISA as described previously.<sup>19</sup> HIV-1

virus stocks were treated with DNase I prior to use for molecular studies. Vpx-containing virus-like particles (VLPs) were generated by transfecting 293T cells with pSIV3+ and the envelope glycoproteins from VSV or A-MLV. SIV p27gag content was determined by ELISA (Zep-tometrix).

## 2.5 | Construction of mutant viruses

HIV-1-BaL-HSA (HIV-1BaL) was used to create  $\Delta$ Vpr,  $\Delta$ Vpu, and  $\Delta$ Vif mutant viruses as described previously.<sup>18</sup> The Vpr R80A and Vpr Q65R mutant viruses were generated by site-directed mutagenesis (Agilent). All mutations were confirmed by sequencing.

## 2.6 | HIV-1 infections

To assess viral replication, MDMs ( $5 \times 10^5$  cells/well in 24-well plates) were incubated with VSV-G-pseudotyped DHIV3-nanoLuc, VSV-G-pseudotyped DHIV3-GFP reporter virus, VSV-G-pseudotyped DHIV3-mCherry reporter virus, or HIV-1<sub>BaL</sub> (125  $\mu$ g p24 per  $5 \times 10^5$  cells) for 4 h at 37°C. Cells were washed 4–5 times with PBS to remove unbound virus and cultured in growth medium. In some cases, infection with HIV-1 was preceded by treatment with Vpx VLPs for 4 h at 37°C. At the indicated times postinfection, cell supernatants were harvested to measure nanoluciferase activity using Nano-Glo luciferase reagent (Promega) or p24 expression by p24<sup>ELISA</sup> ELISA. Alternatively, cells were harvested and GFP or mCherry expression was monitored by flow cytometry using a BD X-20 flow cytometer and analyzed using FlowJo software.

## 2.7 | Enrichment of HIV-1 infected cells

MDMs ( $1.2 \times 10^7$ ) were infected with NL4-3-BaL-IRES-HSA at a multiplicity of infection (MOI) of 2 for 4 h at 37°C, washed 4–5 times with PBS to remove unbound virus, and then cultured in growth medium for 3–6 days. At day 3 or 6 postinfection, MDMs were incubated in PBS with 20 mM EDTA for 2 h at 4°C to remove them from plates and then incubated with PE-conjugated anti-murine CD24 (eBioscience) or biotin-conjugated anti-murine CD24 (eBioscience). Infected (mCD24-positive) MDMs were separated from uninfected (mCD24-negative) using the EasySep Release Human PE Positive Selection kit or the Easy-Sep Release Human Biotin Positive Selection Kit (StemCell Technologies) per the manufacturer's instructions. MDMs were replated and cultured for an additional 18–21 days. HIV-1 replication was assessed by flow cytometry at days 3 (or 6) and 24 postinfection.

## 2.8 | Chromatin immunoprecipitation assays

$1.2 \times 10^7$  MDMs in 10-cm dishes were incubated with VSV-G-pseudotyped DHIV3-GFP reporter virus at an MOI of 2 for 4 h at

37°C. Cells were washed 4–5 times with PBS to remove unbound virus and cultured in growth medium. At days 6 or 24 postinfection, MDMs were fixed in 1% formaldehyde, quenched with 125 mM glycine, and lysed in SDS lysis buffer (1% SDS, 10 mM EDTA, 50 mM Tris pH 8.1, 1 mM PMSF, 1  $\mu$ g/ml aprotinin, 1  $\mu$ g/ml pepstatin A). Cellular lysates were sonicated to fragment the chromatin to an average length of approximately 1000 bp. Samples were diluted and immunoprecipitated with antibodies against NF- $\kappa$ B p65 (EMD Millipore), RNA polymerase II (Santa Cruz Biotechnology), Cyclin T1 (Cell Signaling Technology), or rabbit IgG (Santa Cruz Biotechnology). Purified DNA samples from both chromatin immunoprecipitation (ChIP) and input controls were analyzed quantitatively PCR using the PowerUp SYBR Green Master Mix (ThermoFisher) on a LightCycler L480 (Roche). Primers used to amplify specifically the HIV-1 5' LTR and GLS were 5'-TGGAAGGGCTAATTTACTCCC-3' (forward) and 5'-CATCTCTCCTTCTAGCCTC-3' (reverse). Control amplifications of a serial dilution of either purified U1 genomic DNA or purified pNL4-3 plasmid DNA were performed with each primer set in order to ensure that all amplifications were within the linear range of the reaction. To calculate the relative levels of association with the LTR, the amounts of PCR product obtained for immunoprecipitated chromatin samples were normalized against the amounts of PCR product obtained for input DNA (% Input). All values represent the average of at least 3 independent experiments.

## 2.9 | Analysis of HIV-1 transcription

Total cytoplasmic RNA was isolated from MDMs using the RNeasy Mini kit (Qiagen). HIV-1 RNA was analyzed using the QuantiTect SYBR Green RT-PCR kit (Qiagen) in a LightCycler 480 (Roche). The HIV-1 primers were specific for the R and U5 regions of the LTR and amplify both spliced mRNAs and genomic RNA. The HIV-1 primers were 5'-GGCTAACTAGGGAACCCACTGC-3' (forward) and 5'-CTGCTAGAGATTTCCACACTGAC-3' (reverse). The HIV-1 primers used to analyze transcriptional initiation and elongation included: initiated short transcripts (TAR), 5'-GTTAGACCAGATCTGAGCCT-3' (forward) and 5'-GTGGTTCCTAGTTAGCCA-3' (reverse); and elongated transcripts (*tat* exon 1), 5'-ACTCGACAGAGGAGCAAG-3' and 5'-GAGTCTGACTGTTCTGATGA-3'. The  $\alpha$ -tubulin primers were 5' CACCCGTCTTCAGGGCTTCTGGTTT-3' (forward) and 5' CATTTCACCATCTGGTTGGCTGGCTC-3' (reverse). RNA standards corresponding to 500, 50, and 5 ng of RNA from activated MDMs were included in each experiment to ensure that all amplifications were within the linear range of the assay.

## 2.10 | Detection of total HIV-1 DNA and integrated HIV-1 DNA

$1 \times 10^6$  MDMs were incubated with VSV-G pseudotyped DHIV3-GFP for 4 h at 37°C, washed 4–5 times with PBS to remove unbound virus, and cultured in growth medium for 6 or 24 days. Total DNA was isolated from MDMs using the DNeasy blood and tissue kit (Qiagen)

following the manufacturer's instructions. Total cell-associated HIV-1 DNA was analyzed using the PowerUp SYBR green Master Mix (ThermoFisher) with HIV-1 primers (5'-TTA AGC CTC AAT AAA GCT TGC C-3' R (forward) and 5'-GTT CGG GCG CCA CTG CTA GA-3' (reverse)) and  $\beta$ -globin primers (5'-CCC TTG GAC CCA GAG GTT CT-3' (forward) and 5'-CGA GCA CTT TCT TGC CAT GA-3' (reverse)). Integrated HIV-1 DNA was quantified with the Alu-GAG assay. Briefly, isolated genomic DNA was amplified using human Alu and HIV-1 GAG sequence primers (ALU 5' GCC TCC CAA AGT GCT GGG ATT ACA G-3' (forward) and GAG 5' GTT CCT GCT ATG TCA CTT CC-3' (reverse)) with AmpliTaq Gold DNA polymerase (PerkinElmer) to amplify integrated HIV-1 DNA. Subsequently, amplified HIV-1 DNA was quantified using PowerUp SYBR Green Master Mix (ThermoFisher) with HIV-1 primers (5'-TTA AGC CTC AAT AAA GCT TGC C-3' R (forward) and 5'-GTT CGG GCG CCA CTG CTA GA-3' (reverse)) on a LightCycler 480 (Roche). Control amplifications of a serial dilution of either purified U1 genomic DNA or purified pNL4-3 plasmid DNA were performed with each primer set to ensure that all amplifications were within the linear range of the reaction.

### 2.11 | Analysis of HIV-1 chromatin structure

Restriction enzyme digestions of purified nuclei with *EcoRV* or *AflIII* were performed as described<sup>28,29</sup>. Purified DNA (30  $\mu$ g) was digested to completion with *PstI*. The fragments were analyzed using the Power Up SYBR Green Master Mix (ThermoFisher) in a LightCycler L480 (Roche) with the following primers: Nuc-0 5'-GACAAGAGATCC TTGATCTGTGG-3' (forward) and 5'-GCTAGGAGGCTGTCAAAC TTCCAC-3' (reverse); Nuc-1 5'-TGGCGAGCCCTCAGATGCTAC-3' (forward) and 5'-GTTAGACCAGATCTGAGCCTGGG-3' (reverse) or 5'-GTTCCGGGCGCCACTGCTAGAG-3' (reverse).

### 2.12 | Single cell RNA sequencing

MDMs ( $2 \times 10^6$ ) were spinoculated with A-MLV-pseudotyped DHIV3-mCherry (MOI of 2) in the presence of 10  $\mu$ g/mL polybrene (Millipore) for 2 h at room temperature. MDMs were washed 4–5 times with PBS to remove unbound virus and cultured in growth medium for 7 days. At day 7 postinfection, MDMS were gently detached from plates and resuspended at 1000 cells/ $\mu$ l in PBS with 0.4% BSA. scRNAseq was performed on the 10x Genomics platform using the 5' Gene Expression reagent kit according to the manufacturer's instructions. Gene expression libraries were sequenced on the NovaSeq 6000 Illumina platform to obtain 150-bp paired-end reads at a depth of 200 million total read pairs. The raw gene sequencing data were processed using the 10x Genomics Cell Ranger software (v3.1.0) and analyzed using Loupe Browser 5.0 (10x Genomics). Data were further analyzed using databases available through Interferome.org with the following settings: IFN type: I, II, and III; subtype: all; treatment concentration: any; treatment time: any; in vivo/in vitro: all; species: human; system:

hematopoietic/immune; organ: all; cell: all; cell lines: all; sample types: any.

### 2.13 | shRNA knock-down of MAVS and STING

MDMs ( $1.2 \times 10^7$ ) were infected with retroviruses encoding shRNAs directed against MAVS, STING, or a control shRNA (Sigma) and a puromycin-resistance gene in the presence of Vpx. Infected cells were selected by culture in the presence of puromycin for 5 days, and either used in HIV-1 replication assays or lysed for immunoblot analysis to measure MAVS and STING expression using antibodies to MAVS (Cell Signaling Technology), STING (ProteinTech), vinculin (Cell Signaling Technology), or  $\beta$ -actin (Sigma).

### 2.14 | SDS-PAGE and western blotting

$1 \times 10^6$  MDMs were lysed in 100  $\mu$ l of NETN buffer (100 mM NaCl, 20 mM Tris-Cl pH 8.0, 0.5 mM EDTA, 0.05% NP-40) with protease inhibitors (cOmplete; Roche) and phosphatase inhibitor (PhosphoStop; Roche), and protein concentration was determined using BCA protein assay kit (Pierce). Proteins were separated on SDS-PAGE gels and transferred to PVDF membranes (Millipore). Membranes were probed with antibodies to MAVS (Cell Signaling Technology), STING (ProteinTech), vinculin (Cell Signaling Technology), or  $\beta$ -actin (Sigma), developed using Western Lightening Chemiluminescent Substrate (PerkinElmer), and analyzed in a ChemiDoc imager (Bio-Rad Laboratories).

### 2.15 | IFN- $\beta$ ELISA

IFN- $\beta$  in cell-culture supernatant was measured using the VeriKine-HS Human IFN- $\beta$  Serum ELISA Kit (PBL Assay Science) following the manufacturer's instructions.

### 2.16 | Viability assays

Cell viability of uninfected and HIV-1-infected MDMs was monitored over time (longitudinal) and at the end of culture (endpoint) using CytoTox-One Homogeneous Membrane Integrity Assay or CytoTox-Glo kits (Promega) per the manufacturer's instructions.

### 2.17 | Statistical analysis

Comparison between experimental samples was performed with a paired two-tailed *t*-tests or Fishers exact tests with  $p < 0.05$  denoting significant differences. Experiments were performed in triplicate using cells from a minimum of 4 independent donors (unless otherwise indicated) to control for interdonor variability.

### 3 | RESULTS

#### 3.1 | HIV-1 enters a state reminiscent of viral latency in macrophages

Latently infected cells represent the major barrier to a cure for HIV-1 infection. Latent HIV-1 infection, in which replication-competent integrated provirus enters a reversible transcriptionally silent state, has been demonstrated in CD4-positive memory T cells.<sup>2-4</sup> Although macrophages are known to maintain persistent, low-level infections in vivo,<sup>10,20-25</sup> the existence of a truly latent reservoir in these cells has been debated. To determine whether macrophages can establish and maintain latent HIV-1 infection, we utilized an in vitro MDM model of HIV-1 infection. We infected MDMs with a single-round replication-competent version of HIV-1 that encodes secreted nanoluciferase (DHIV3-nanoluciferase) and is pseudotyped with the glycoprotein of vesicular stomatitis virus (VSV). A single-round replication-competent virus was chosen to synchronize infection and to eliminate the contribution of viral spread in culture. We found that in MDMs from a majority of donors (18 out of 26, 69.2%), HIV-1 replication peaked early after infection—typically between days 3 and 12 postinfection—and steadily decreased over time in culture (Figure 1(A)), with a significant decrease in viral replication between the day of peak replication and the endpoint of culture (Figure 1(B)). In MDMs from a minority of donors (8 out of 26, 30.8%), HIV-1 replication did not significantly decrease during extended time in culture (Figures 1(C) and 1(D)). The observed decrease in HIV-1 replication in MDMs over time in culture was not due to decreased cell viability, as HIV-1-infected MDMs were as viable as uninfected MDMs (Figure 1(E)). Recent studies have demonstrated that there are sex-based differences in HIV-1 infection of macrophages,<sup>26</sup> but the observed decrease in HIV-1 replication in MDMs was independent of donor sex (Figure 1(F)). We analyzed MDMs from 26 donors, including 13 male donors and 13 female donors. Of the 18 donors whose MDMs supported latent infection, 11 were male and 7 were female. Of the 8 donors whose MDMs did not support latent infection, 2 were male and 6 were female. The ability of HIV-1 to enter latency in MDMs was correlated with the degree of peak virus replication as MDMs with higher peak levels of virus replication were more likely to exhibit a significant decrease in virus replication over time, whereas MDMs that supported a lower peak of virus replication maintained a more sustained level of replication (Figure 1(G)), indicating that cells with higher virus replication peaks were more likely to enter a latent-like state. Latently infected cells are characterized by intact, replication-competent provirus in the absence of viral transcription that can be reactivated by LRAs. We found that MDMs exhibiting decreased viral replication over time in culture demonstrated reduced or absent viral transcription (Figure 1(H)). In addition, MDMs with decreased HIV-1 replication and transcription did not contain significantly lower levels of total cell-associated HIV-1 DNA or integrated proviral DNA (Figures 1(I) and 1(J)). Finally, treating HIV-1-infected MDMs with LRAs near the end of their time in culture led to increased replication (Figure 1(K)),

consistent with viral reactivation at a population level. Although the method used to detect integrated HIV-1 proviral DNA in these experiments cannot differentiate between full-length, replication-competent provirus and truncated, replication-defective provirus, the ability of LRAs to reactivate HIV-1 replication suggests that there was full-length replication-competent virus in the latently infected cells. The studies discussed above utilized a single-round, replication-competent virus that lacks the *env* gene. To determine whether a similar phenotype would be observed if MDMs were infected with replication-competent, macrophage-tropic HIV-1, we infected MDMs with HIV-1<sub>BaL</sub> and observed viral replication levels over time. We found that MDMs from a subset of donors (8 out of 10 donors) infected with replication-competent HIV-1 demonstrated a similar course of viral replication with a peak early after infection followed by decreased viral replication in the absence of significant cell death (Figures 1(L) and 1(M)). Taken together, these findings suggest that in MDMs from a subset of donors, HIV-1 enters a state reminiscent of viral latency.

Our results demonstrated that HIV-1 can enter a state of viral latency in MDMs at a population level. In order to determine whether HIV-1 enters latency in MDMs at a single-cell level, we employed 2 strategies. First, we infected MDMs with a single-round replication-competent version of HIV-1 that encodes GFP (DHIV3-GFP) or mCherry (DHIV3-mCherry) pseudotyped with the VSV glycoprotein and observed GFP or mCherry expression over time using flow cytometry as a proxy for HIV-1 replication. The number of HIV-positive cells decreased over time in culture, consistent with a transition to a latent state (Figures 2(A) and 2(B)). The decrease in viral replication in these cells was not due to decreased viability (Figures 2(C)). This effect was even more pronounced when infection levels were increased by pre-treating MDMs with Vpx to deplete SAMHD1<sup>27</sup> prior to infection with DHIV-GFP. In these MDMs, HIV-1 replication decreased over time in culture and was reversible on a single cell level by treatment with LRAs such as TNF- $\alpha$  or PMA (Figure 2(D)). Second, we infected MDMs with a version of HIV that encodes murine CD24 (HIV-mCD24), sorted cells at day 3 or 6 postinfection to enrich for HIV-1 positive cells, and measured HIV-1 replication by flow cytometry over time in culture (Figure 2(E)). We observed a significant decrease in HIV-mCD24-infected MDMs over time in culture, from an average of  $83.98 \pm 8.45\%$  mCD24-positive MDMs at day 3 or 6 postinfection to an average of  $25.92 \pm 2.49\%$  mCD24-positive MDMs at day 24 postinfection (Figure 2(F)), without a decrease in viability (Figure 2(G)). Latent HIV-1 in these MDMs was also reactivated by treatment with TNF- $\alpha$  or PMA (Figure 2(H)), with an average of  $10.69 \pm 4.49\%$  of TNF- $\alpha$ -treated MDMs expressing mCD24 and  $19.60 \pm 14.57\%$  of PMA-treated MDMs expressing mCD24 compared with just  $2.14 \pm 1.51\%$  in untreated MDMs. Of note, it is possible that the negative fraction of MDMs (Figure 2(E)) contains cells with integrated, intact HIV-1 proviral DNA that have entered latency early after infection, as has been observed in other in vitro MDM models of viral latency.<sup>16</sup> Taken together, these findings suggest that in MDMs from a subset of donors, HIV-1 enters a state reminiscent of viral latency.

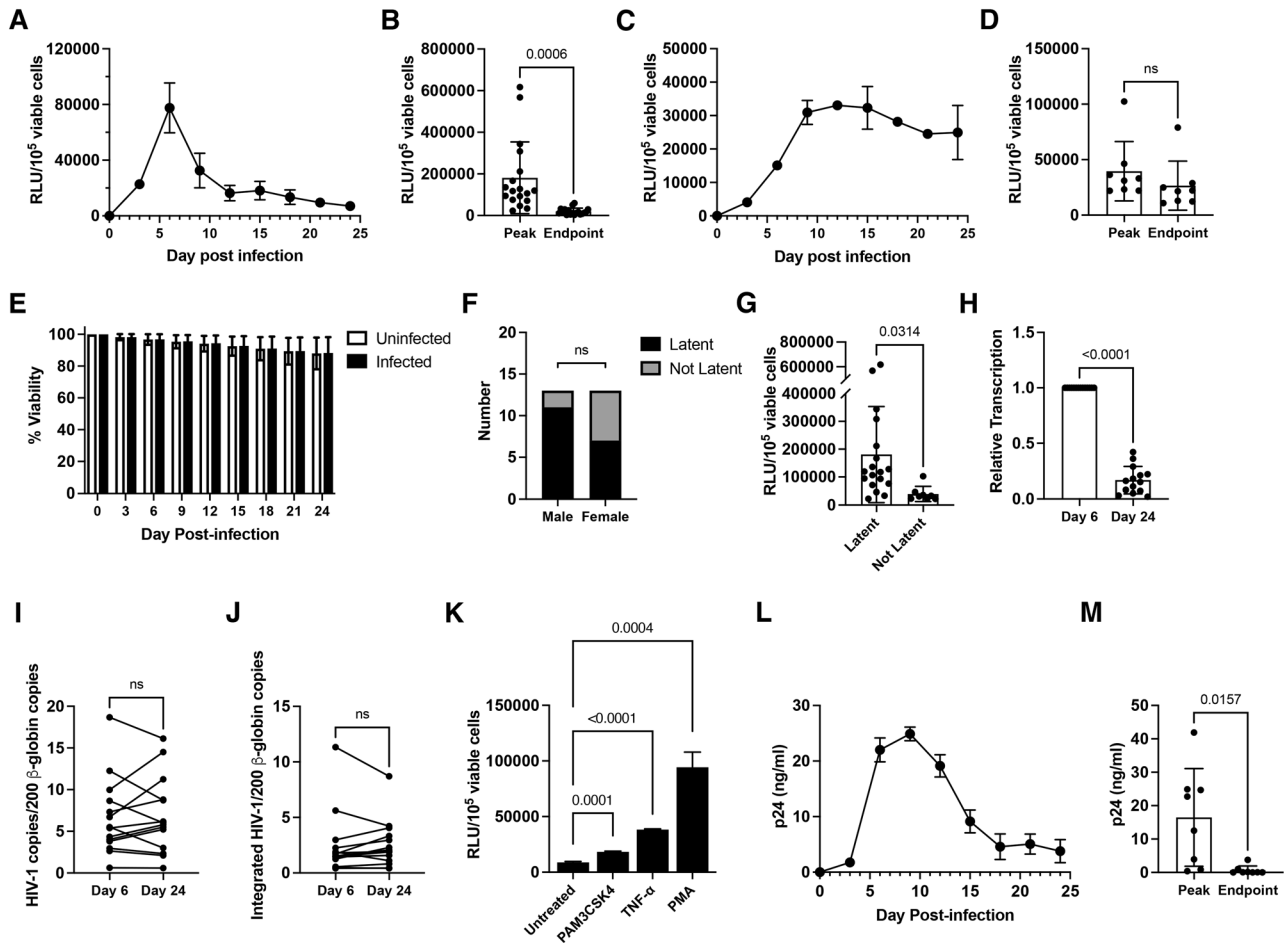


**FIGURE 1** HIV-1 enters a state resembling latency in MDMs during extended time in culture. (A–D). MDMs ( $5 \times 10^5$  cells/well) were infected with VSV-G-pseudotyped DHIV3-nanoluciferase and cultured for up to 24 days. Culture supernatant was sampled every 3 days and viral replication was measured by nanoluciferase activity. Viral replication in MDMs from 1 representative donor (A and C) and comparison of peak and endpoint viral replication in MDMs from all donors (C and D) are shown. (E) Viability of MDMs infected and cultured as in (A). (F) Comparison of MDM donor sex demonstrating latent and not latent viral replication. Male donors: 11 latent (black) and 2 not latent (gray). Female donors: 7 latent (black) and 6 not latent (gray). (G) Comparison of peak replication levels in MDMs demonstrating latent and not latent viral replication. (H) MDMs ( $1 \times 10^6$ /well) were infected as in (A), and cytoplasmic RNA was isolated at days 6 and 24 postinfection. HIV-1 transcription was measured by RT-qPCR. (I and J) MDMs ( $1 \times 10^6$ /well) were infected as in (A). Cellular DNA was isolated at days 6 and 24 postinfection. Total (I) and integrated (J) HIV-1 DNA was measured by qPCR. (K) MDMs were infected as in (A) and cultured for 24 days. At day 24 postinfection, MDMs were treated with PAM3CSK4 (100 ng/ml), TNF- $\alpha$  (50 ng/ml), PMA (100 nM), or vehicle control. Culture supernatant was sampled 3 days after treatment and viral replication was measured by nanoluciferase activity. (L and M) MDMs ( $5 \times 10^5$  cells/well) were infected with replication competent HIV-1<sub>BaL</sub> and cultured for up to 24 days. Culture supernatant was sampled every 3 days and viral replication was measured by p24 ELISA. Viral replication in MDMs from 1 representative donor (L) and comparison of peak and endpoint viral replication in MDMs from all donors (M) are shown. Statistical analysis: two-tailed *t*-test (B, D, E, H, I, J, K, M); one-tailed *t*-test (G), and Fisher's exact test (F)

### 3.2 | The transition to HIV-1 latency in macrophages is associated with changes in transcription factor recruitment to the LTR

Previous studies from our laboratory showed that coinfection of MDMs with certain bacteria that induce type I IFN production induce HIV-1 latency by altering transcription factor recruitment to the HIV-1 5' LTR.<sup>15</sup> We wanted to determine whether the transition to latency in HIV-1 infected MDMs we observed over time was associated with changes in transcription factor recruitment to the viral promoter. Using ChIP, we found that during early points after infection, when viral repli-

cation and transcription in MDMs was robust, the p65 subunit of NF- $\kappa$ B was associated with the viral promoter (Figure 3(A)). In addition, RNA polymerase II and Cyclin T1, a component of p-TEFb, were also associated with the LTR. However, after an extended period of time in culture, there was a dramatic decrease in the association of NF- $\kappa$ B p65, RNA polymerase II, and Cyclin T1 with the LTR, which corresponded to the significant decrease in HIV-1 replication and transcription (Figure 1).

During infection, the HIV-1 provirus integrates into cellular genomic DNA and is packaged into chromatin such that the 5'-LTR is bound by 2 positioned nucleosomes, nucleosome 0 (Nuc-0) and nucleosome 1 (Nuc-1).<sup>28,29</sup> Nuc-1 is thought to play a role in the restriction of HIV-1

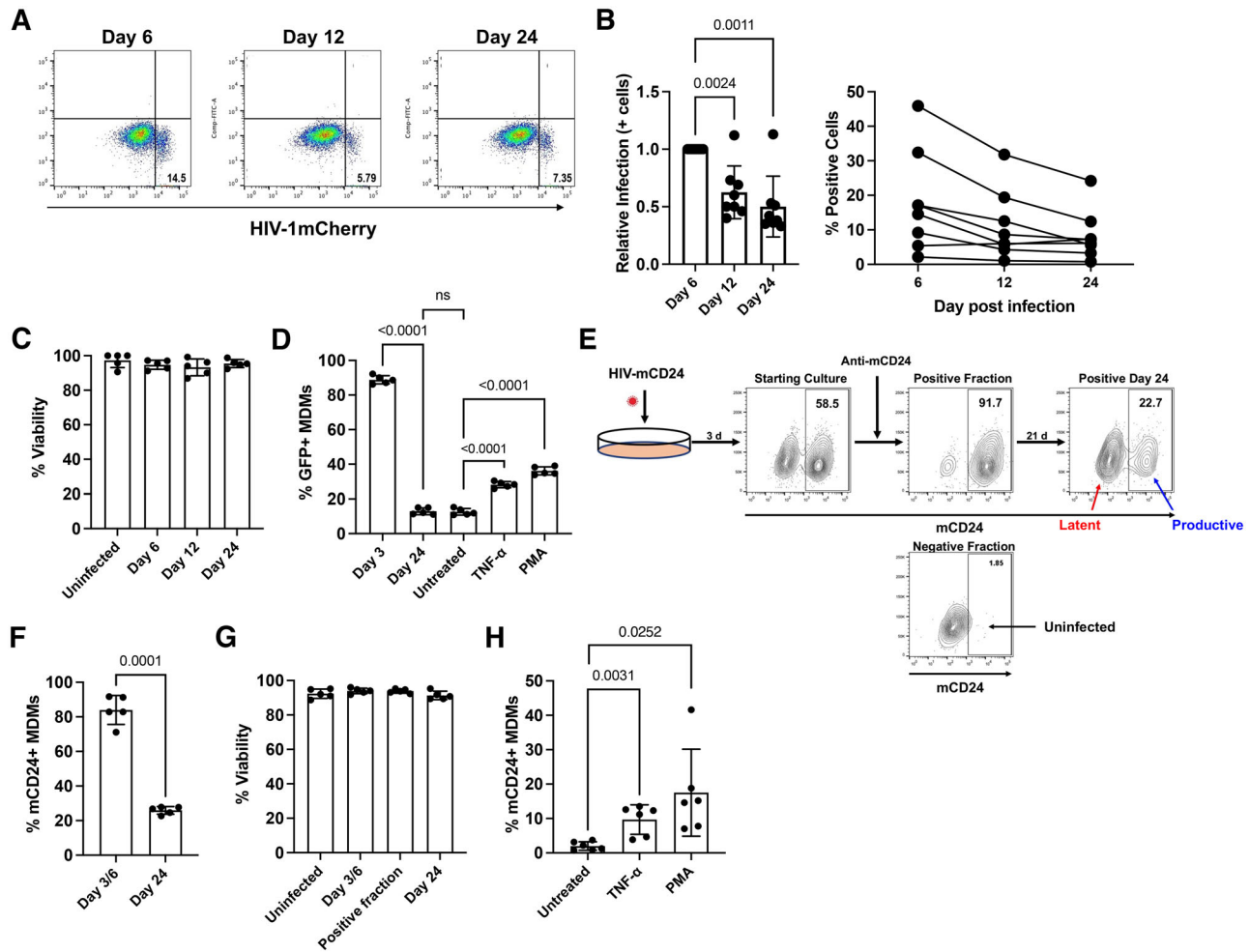


**FIGURE 2** HIV-1 enters a latent state in individual MDMs. (A and B) MDMs ( $5 \times 10^5$  cells/well) were infected with VSV-G-pseudotyped DHIV3-GFP or VSV-G-pseudotyped DHIV3-mCherry and cultured for up to 24 days. Cells were sampled at the indicated days postinfection and viral replication was measured by flow cytometry. Viral replication in MDMs from 1 representative donor (A) and comparison of viral replication in MDMs from all donors (B) are shown. (C) Viability of HIV-1 infected and uninfected MDMs was monitored during culture. (D) MDMs ( $5 \times 10^5$  cells/well) were treated with Vpx VLPs and subsequently infected with VSV-G-pseudotyped DHIV3-GFP and cultured for up to 24 days. At day 24 postinfection, MDMs were treated with TNF- $\alpha$  (50 ng/ml), PMA (100 nM), or vehicle control. Viral replication was measured by flow cytometry. (E and F) MDMs ( $1.2 \times 10^7$  cells) were infected with HIV-1<sub>BAL</sub> expressing murine CD24 and sorted at day 3 or 6 postinfection to enrich for HIV-1-infected MDMs. Sorted MDMs were cultured for an additional 18–21 days and viral replication was measured by flow cytometry. One representative donor is shown (E) and composite data from 5 donors are shown (F). (G) Viability of HIV-1 infected and uninfected MDMs was monitored during culture. (H) A subset of sorted MDMs were treated at day 24 with TNF- $\alpha$  (50 ng/ml), PMA (100 nM), or vehicle control and viral replication was measured by flow cytometry. Statistical analysis: two-tailed *t*-test (B, C, D, F, G, and H)

transcription in latently infected cells and must be remodeled prior to transcription.<sup>28–30</sup> To determine whether the chromatin structure at the HIV-1 promoter was altered during the transition to viral latency, we used nucleosome accessibility assays and found that Nuc-1 was remodeled in MDMs early after infection, but it was not remodeled at later time points postinfection when HIV-1 expression is decreased (Figure 3(B)). In T cells, HIV-1 latency is thought to occur as a result of an inhibition of transcriptional elongation.<sup>31–33</sup> In contrast to the above observations in T cells, we found that latency in MDMs is associated with a block to transcriptional initiation, as there was a significant decrease in both early initiated transcripts and elongated transcripts (Figure 3(C)). These data suggest that the recruitment of NF- $\kappa$ B, a transcription factor known to be essential for HIV-1 transcription

in macrophages, decreases over time and leads to a concomitant decrease in the recruitment of RNA polymerase II and p-TEFb, a failure to remodel Nuc-1, and a block to transcription initiation. Together, these findings suggest that viral latency is associated with changes to the recruitment of transcription factors to the HIV-1 promoter, and a resulting block to transcription initiation and chromatin remodeling.

### 3.3 | Type I IFN signaling promotes HIV-1 latency in macrophages

HIV-1 infection of macrophages leads to the generation of an innate immune response<sup>34</sup> characterized by the production of type I IFNs and

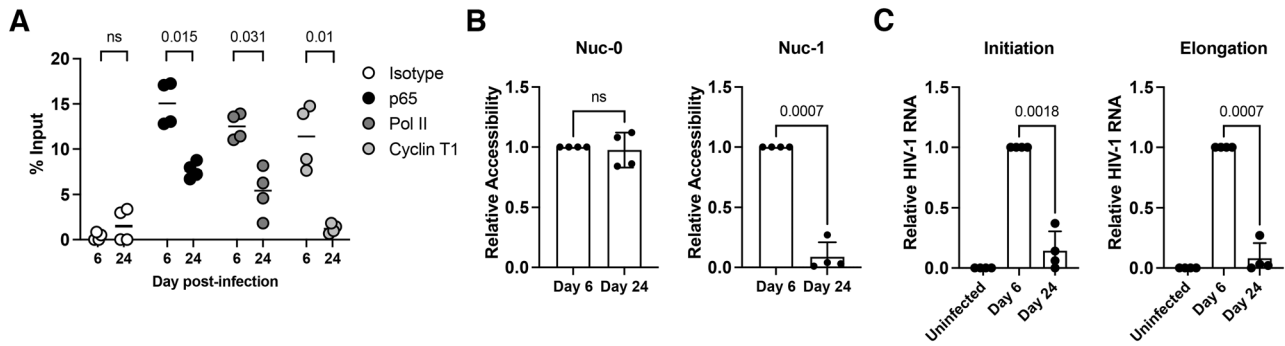


**FIGURE 3** Latent HIV-1 infection in MDMs is associated with changes in transcription factor recruitment and chromatin structure at the 5' LTR. (A) MDMs ( $1.2 \times 10^7$  cells) were infected with VSV-G-pseudotyped DHIV3-GFP and cultured for up to 24 days. Cells were harvested at day 6 or 24 postinfection, fixed with formaldehyde, lysed, sonicated, and subjected to immunoprecipitation with antibodies against NF- $\kappa$ B p65, RNA polymerase II, Cyclin T1, or rabbit IgG (isotype control). Association with the HIV-1 5' LTR was assessed by PCR using HIV-1 specific primers. (B) MDMs were infected as in (A) and cultured for up to 24 days. At day 6 or 24 postinfection, nuclei were prepared from the cells and digested with *EcoRV* or *AflIII* to evaluate accessibility at Nuc-0 and Nuc-1, respectively. (C) MDMs ( $1 \times 10^6$ /well) were infected as in (A), and cytoplasmic RNA was isolated at days 6 and 24 postinfection. HIV-1 transcription was measured by RT-qPCR. Transcription initiation was measured using primers for TAR and transcription elongation was measured using primers for *tat* exon 1 as described previously.<sup>63</sup> Statistical analysis: two-tailed t-test (A, B, and C)

the expression of numerous IFN-regulated genes (IRGs).<sup>35</sup> We sought to determine whether the induction of a type I IFN response in MDMs was necessary for the establishment of latent HIV-1 infection. Treatment of HIV-1-infected MDMs with IFN- $\alpha$  or IFN- $\beta$  was sufficient to induce a state of viral latency in MDMs (Figure 4(A)), similar to our previous findings demonstrating that co-infections that induce type I IFNs promote HIV-1 latency in MDMs.<sup>15</sup> To further confirm the importance of type I IFNs in the establishment of viral latency, HIV-1-infected MDMs were cultured in the presence of the soluble type I IFN inhibitor, B18R, (Figure 4(B)) or in the presence of chemical inhibitors of type I IFN signaling (Figure 4(C)). Inhibition of type I IFN signaling prevented the establishment of latent viral infections in MDMs. This was associated with increased levels of NF- $\kappa$ B p65 and RNA polymerase II at the viral promoter (Figure 4(D)) and remodeling of Nuc-1 (Figure 4(E)) late in infection in MDMs treated with B18R. These data suggest that type I IFN signaling is required for the transition to latency in macrophages.

To further evaluate the role of type I IFN signaling in the establishment of latent HIV-1 infection in macrophages, we performed single-cell RNA sequencing of HIV-1-infected MDMs at day 7 postinfection to obtain a snapshot of gene expression as MDMs transitioned to a state of viral latency. When comparing HIV-1-infected MDMs to uninfected MDMs in parallel culture, we found that there were 906 differentially expressed genes (DEGs) (Figure 4(F)). Of these 326 (36%) were bona fide IRGs (Figure 4(G)), demonstrating that IRGs are enriched in the setting of HIV-1 infection. These IRGs include IFN- $\beta$ , as well as a number of known antiviral proteins including APOBEC3A,<sup>36</sup> IDO1,<sup>37</sup> and IFI27.<sup>38</sup> When comparing MDMs with high levels of virus expression to MDMs with low levels of virus expression in the same culture (Figure 4(H)), we found that of the 71 DEGs, 49 (69%) were IRGs (Figure 4(I)). These DEGs are listed in Table S1. These findings suggest that expression of IRGs is associated with the transition to latency.

### 3.4 | MAVS signaling is essential for the establishment of latent HIV-1 infection of MDMs

Multiple studies have demonstrated that HIV-1 can be sensed by a diverse set of innate immune receptors including TLR3,<sup>39</sup> TLR7,<sup>40,41</sup> TLR8,<sup>40,42</sup> TLR9,<sup>41</sup> RIG-I,<sup>43</sup> cGAS,<sup>44</sup> and PKR<sup>45</sup> leading to the production of type I IFNs. We wished to determine whether sensing of HIV-1 by these signaling pathways contributed to the establishment of latency in MDMs. Pharmacologic inhibition of TBK1, a kinase downstream of the TLR, RIG-I/MDA5/MAVS, and cGAS/STING signaling pathways, partially prevented the establishment of HIV-1 latency in MDMs (Figure 5(A)). This partial block to latency induction was possibly due to the need to use a suboptimal concentration of the TBK1 inhibitor BX795 to prevent cytotoxicity. Regardless, these data suggest that one or more of the signaling pathways that employ TBK1 contributes to viral latency in MDMs. Long-term culture of HIV-1-infected MDMs in the presence of inhibitors of TLR3, TLR7/8, and PKR did not prevent the establishment of viral latency (Figure 5(B)). Inhibition of endosomal acidification with bafilomycin A1, which prevents signaling through endosomal TLRs, also did not prevent the transition to latency (Figure 5(B)). In addition, culture of MDMs in the presence of cGAS and STING inhibitors (Figure 5(C)) did not block the establishment of latency, suggesting that the detection of HIV-1 DNA by the cGAS/STING pathway is not important for the establishment of HIV-1 latency in MDMs. Since there are no available pharmacologic inhibitors for RIG-I, MDA5, or MAVS, we utilized shRNA knockdown of MAVS to investigate the role of the RIG-I/MDA5/MAVS pathway in HIV-1 latency. As shown in Figure 5(D)), we could efficiently knockdown expression of STING or MAVS using shRNA in MDMs. Knockdown of MAVS and STING did not affect subsequent infection of MDMs with HIV-1 (Figure 5(E)), most likely



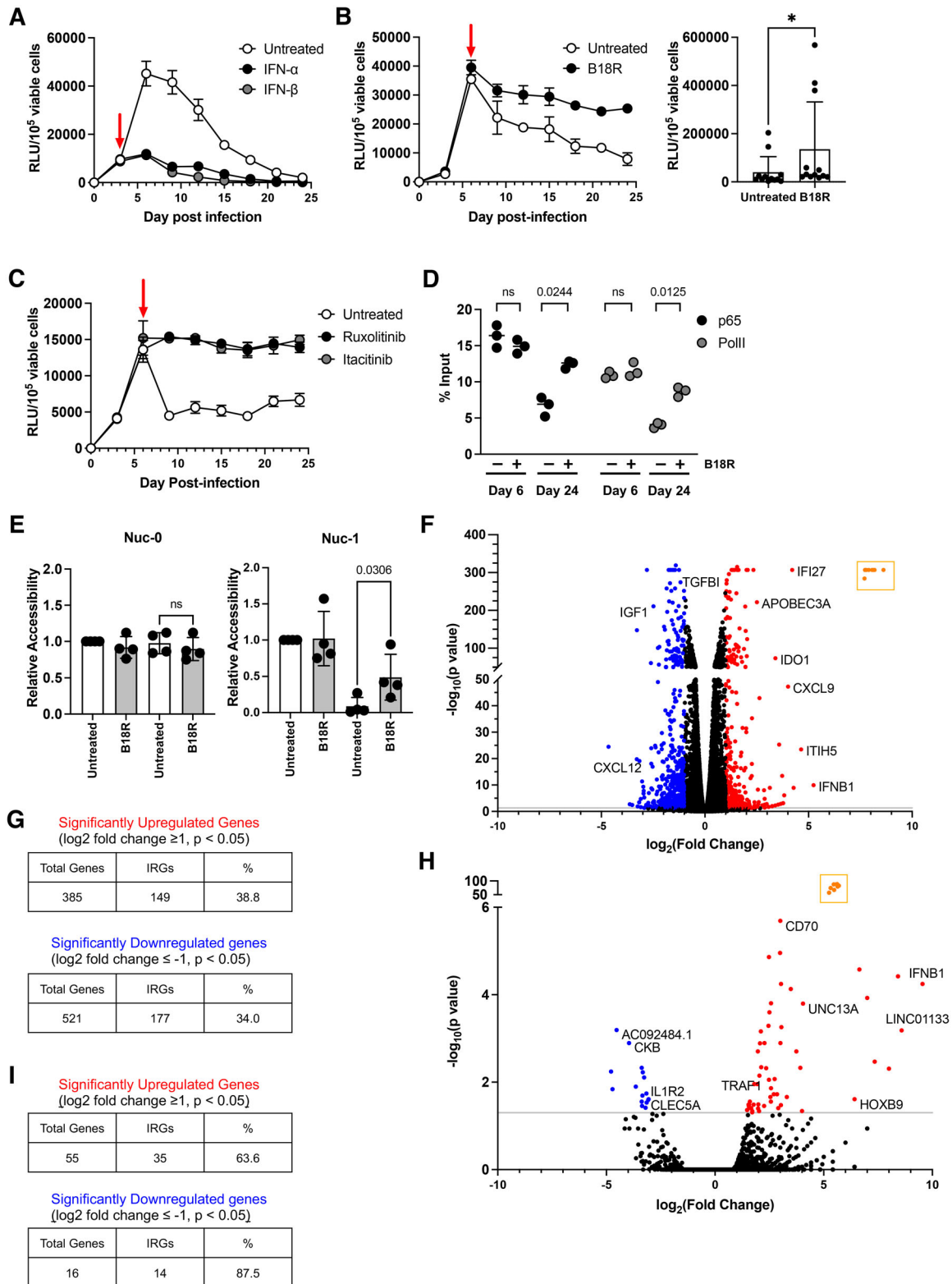


**FIGURE 4** HIV-1 latency is induced by type I IFN signaling. (A) MDMs ( $5 \times 10^5$ /well) were infected with VSV-G-pseudotyped DHIV3-nanoluciferase and cultured for up to 24 days. MDMs were treated with a single dose of IFN- $\alpha$  or IFN- $\beta$  at day 3 postinfection. Viral replication was measured by luciferase assay. Data from 1 representative donor (of 3) are shown. (B) MDMs ( $5 \times 10^5$  cells/well) were infected with VSV-G-pseudotyped DHIV3-nanoluciferase and cultured for up to 24 days in the absence or presence of the soluble type I IFN inhibitor, B18R (100 ng/ml), starting at day 6 postinfection. Viral replication was measured by nanoluciferase assay. Data from 1 representative donor and composite endpoint data from 12 donors are shown. (C) MDMs were infected as in (B) and cultured for up to 24 days in the absence or presence of ruxolitinib (10  $\mu$ M), itacitinib (10  $\mu$ M), or vehicle control starting at day 6 postinfection. Viral replication was measured by nanoluciferase assay. Data from 1 representative donor (of 5) are shown. (D) MDMs ( $1.2 \times 10^7$  cells) were infected with VSV-G-pseudotyped DHIV3-GFP and cultured

(Continues)

**FIGURE 4** (Continued)

for up to 24 days in the absence or presence of B18R (100 ng/ml), starting at day 3 postinfection. Cells were harvested at day 6 or 24 postinfection, fixed with formaldehyde, lysed, sonicated, and subjected to immunoprecipitation with antibodies against NF- $\kappa$ B p65, RNA polymerase II, or rabbit IgG (isotype control). Association with the HIV-1 5' LTR was assessed by PCR using HIV-1 specific primers. (E) MDMs were infected and cultured as in (D). At day 6 or 24 postinfection, nuclei were prepared from the cells and digested with *EcoRV* or *AflIII* to evaluate accessibility at Nuc-0 and Nuc-1, respectively. (F–I) MDMs from 4 donors (2 males and 2 females) were infected with A-MLV-pseudotyped DHIV3-mCherry and cultured for 7 days. At day 7 postinfection, the MDMs were harvested and submitted for scRNASeq. A volcano plot comparing parallel HIV-1-infected and uninfected MDMs is shown in (F). Data from uninfected and infected MDMs were analyzed using the Interferome database to assess for enrichment for IRGs (G). Infected MDMs were stratified by mCherry (HIV-1) mRNA expression. A volcano plot comparing MDMs with high levels of mCherry transcripts and those with low levels of mCherry transcripts is shown in (H). Data from uninfected and infected MDMs were analyzed using the Interferome database to assess for enrichment for IRGs (I). Statistical analysis: two-tailed *t*-test (B, D, and E)

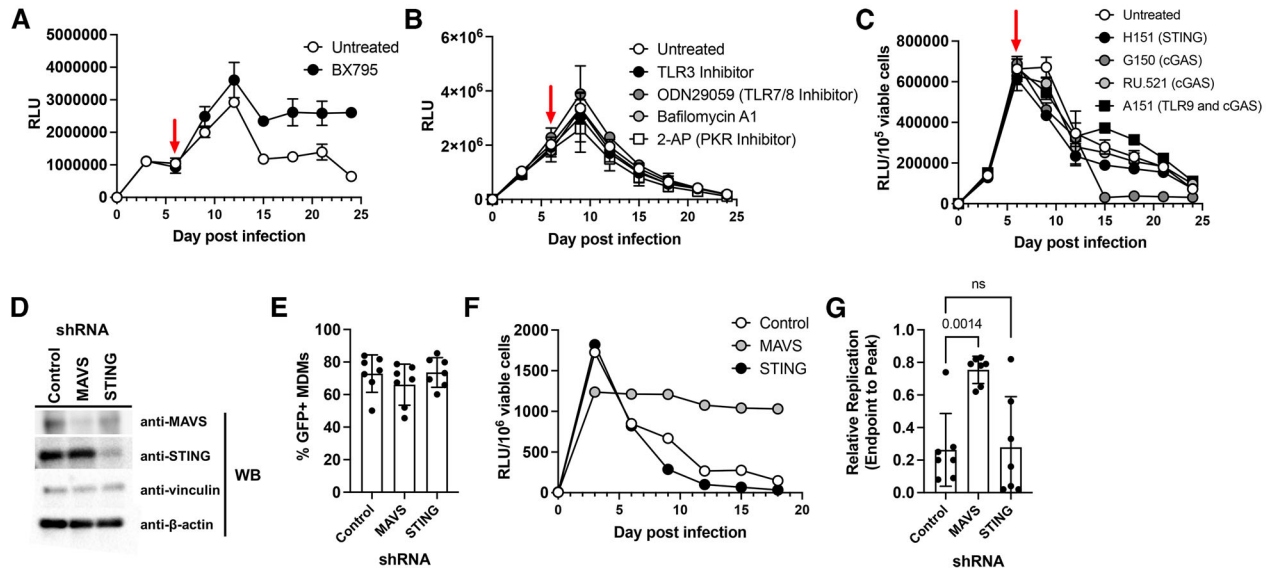


**FIGURE 5** MAVS signaling is required for the establishment of HIV-1 latency in MDMs. (A) MDMs ( $5 \times 10^5$  cells/well) were infected with VSV-G-pseudotyped DHIV3-nanoluciferase and cultured for up to 24 days in the absence or presence of the TBK1 inhibitor, BX795 ( $1 \mu\text{M}$ ) starting at day 6 postinfection. Viral replication was measured by nanoluciferase assay. Data from 1 representative donor (of 5) are shown. (B) MDMs were infected as in (A) and cultured for up to 24 days in the presence or absence of inhibitors to TLR3 (TLR3 inhibitor,  $10 \mu\text{M}$ ), TLR7/8 (ODN 20959,  $5 \mu\text{M}$ ), endosomal acidification (Bafilomycin A1,  $100 \text{ nM}$ ) or PKR (2-AP,  $1 \text{ mM}$ ), starting at day 6 postinfection. Viral replication was measured by nanoluciferase assay. Data from 1 representative donor (of 3) are shown. (C) MDMs were infected as in A and cultured for up to 24 days in the presence or absence of inhibitors to STING (H-151,  $15 \mu\text{M}$ ), cGAS (G150,  $10 \mu\text{M}$  and RU.521,  $48.2 \mu\text{M}$ ), or cGAS/TLR9 (A151,  $10 \mu\text{M}$ ) starting at day 6 postinfection. Viral replication was measured by nanoluciferase assay. Data from 1 representative donor (of 5) are shown. (D–G) MDMs ( $2 \times 10^6$  cells/well) were treated with Vpx VLPs and then infected with retroviral particles encoding the indicated shRNAs and a puromycin resistance gene. MDMs were selected in puromycin for 5 days and knockdown was assessed by immunoblot (D). Puromycin-selected MDMs were then infected with VSV-G-pseudotyped DHIV3-GFP, cultured for 3 days, and analyzed by flow cytometry (E). Puromycin-selected MDMs were infected with VSV-G-pseudotyped DHIV3-nanoluciferase and cultured for up to 18 days. Culture supernatant was sampled every 3 days and viral replication was measured by nanoluciferase activity. Data from 1 representative donor (F) and composite relative replication (ratio of endpoint to peak viral replication) data from 7 donors (G) are shown. Statistical analysis: two-tailed *t*-test (E and G)

due to Vpx-mediated degradation of SAMHD1. While knockdown of STING did not prevent HIV-1 from entering a latent state in MDMs, confirming our results using chemical inhibitors, knock-down of MAVS prevented the establishment of HIV-1 latency in MDMs (Figures 5(F) and 5(G)), suggesting that sensing of either viral RNA or endogenous danger signals by the RIG-I/MDA5/MAVS/TBK1 pathway is essential for the establishment of latent HIV-1 infection in MDMs.

### 3.5 | Vpr induces an attenuated IFN response that contributes to HIV-1 latency

We recently demonstrated that the viral accessory protein Vpr is largely responsible for inducing an attenuated IFN response in MDMs.<sup>18</sup> We sought to determine whether Vpr or other HIV-1 accessory proteins contributed to the establishment of viral latency in MDMs through modulation of type I IFN expression. We found that

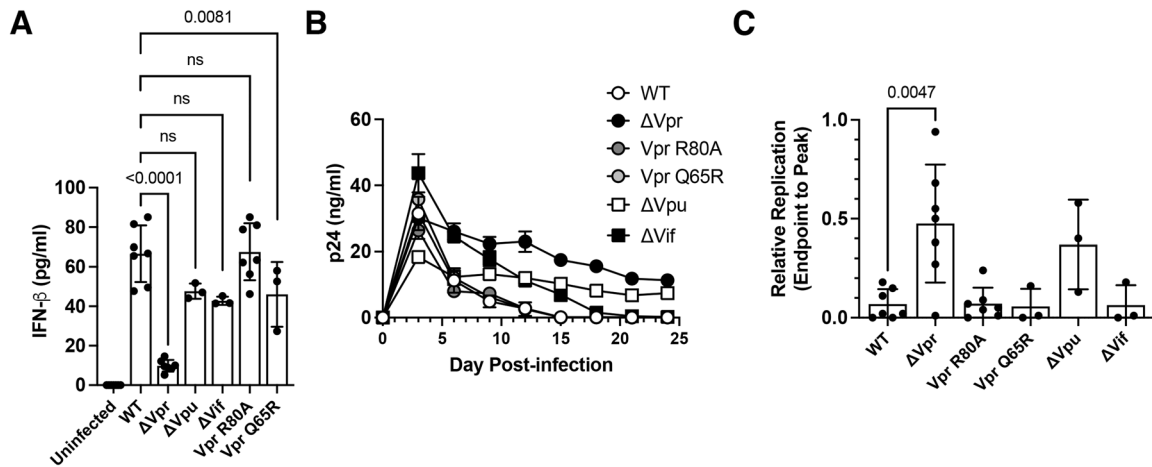


**FIGURE 6** HIV-1 accessory protein Vpr contributes to the establishment of latency. MDMs ( $5 \times 10^5$  cells/well) were infected with wild-type HIV-1<sub>BaL</sub>, HIV-1<sub>BaL</sub> ΔVpr, HIV-1<sub>BaL</sub> ΔVpu, HIV-1<sub>BaL</sub> ΔVif, HIV-1<sub>BaL</sub> Vpr R80A, or HIV-1<sub>BaL</sub> Vpr Q54R and cultured for up to up to 24 days. (A) IFN-β production was measured by ELISA at day 3 postinfection. (B and C) Viral replication was measured by p24 ELISA. Data from 1 representative donor (B) and composite relative replication (ratio of endpoint to peak replication) data from up to 7 donors (C) are shown. Statistical analysis: two-tailed t-test (A)

infection of MDMs with Vpr-deficient HIV-1 failed to induce type I IFN production compared with wild type HIV-1 (Figure 6(A)), consistent with our previous findings.<sup>18</sup> Of note, absence of other HIV-1 accessory proteins, including Vpu and Vif, did not significantly alter type I IFN production in infected MDMs. In addition, the G2/M cell cycle arrest function of Vpr was not necessary for type I IFN induction, as infection of MDMs with HIV-1 harboring the Vpr R80A mutation, which fails to induce G2/M cell cycle arrest, did not significantly alter type I IFN production. Infection with HIV-1 harboring Vpr with the Q65R mutation, which does not bind to DCAF1,<sup>46</sup> led to a small but reproducible decrease in type I IFN production (Figure 6(A)), suggesting a possible role for the E3 ligase Cul4A<sup>DBB1/DCAF1</sup> binding function of Vpr in the induction of type I IFNs. Furthermore, MDMs infected with Vpr-deficient HIV-1 did not progress to a state of latency when compared to MDMs infected with wild type HIV-1 (Figures 6(B) and 6(C)). HIV-1 constructs lacking either Vpu or Vif were able to transition to latent infection, although this transition was delayed in HIV-1 lacking Vpu. This suggests a possible role for Vpu in the establishment of latency (Figures 6(B) and 6(C)). HIV-1 harboring Vpr with R80A or Q65R mutations did transition to latency in MDMs, suggesting that the G2/M cell cycle arrest and DCAF1 binding functions of Vpr, respectively, are not required for the establishment of latency in macrophages. These data suggest that Vpr is necessary for generating an IFN response during HIV-1 infection and contributes to the establishment of latent infection in MDMs.

#### 4 | DISCUSSION

Here, we demonstrate that *in vitro* MDMs infected with HIV-1 are characterized by robust viral replication shortly after infection followed by a steady decrease in viral replication the longer the cells are kept in culture (Figures 1 and 2). Decreased viral replication is associ-

ated with decreased transcription without changes in cell-associated viral DNA or integrated proviral DNA. Viral latency is reversible in these cells upon treatment with LRAs. Although we show that HIV-1 infection in MDMs can transition to a state resembling viral latency *in vitro*, it remains to be seen whether HIV-1 can establish true latent infections in tissue macrophages *in vivo*. Recent studies in human subjects, non-human primates, and humanized mouse models suggest that there is an inducible viral reservoir in tissue macrophages.<sup>10–16</sup> Future studies will examine whether tissue macrophages can serve as a true latent HIV-1 reservoir.

In our studies, we derived MDMs from CD14<sup>+</sup> monocytes, a population that includes both CD14<sup>+</sup> CD16<sup>-</sup> “classical” monocytes and CD14<sup>+</sup>CD16<sup>+</sup> “intermediate” monocytes. This approach potentially excludes a small subset of normal circulating monocytes, “non-classical” CD14<sup>dim</sup>CD16<sup>+</sup> monocytes. Studies have shown that CD16<sup>+</sup> monocytes are more permissive to HIV-1 infection than classical CD14<sup>+</sup>CD16<sup>-</sup> monocytes and may harbor HIV-1 *in vivo*, contributing to the myeloid reservoir.<sup>47–49</sup> It will be important, therefore, to determine whether MDMs derived from the different circulating monocyte subsets have different capacities for harboring latent HIV-1 infection, as well as their respective contributions to the establishment of the myeloid reservoir *in vivo*. In a macaque model, decreasing the frequency of circulating CD14<sup>+</sup>CD16<sup>+</sup> monocytes and CD14<sup>dim</sup>CD16<sup>+</sup> monocytes did not alter the establishment of the SIV tissue reservoir.<sup>50</sup>

The transition to a latent state is associated with changes in the recruitment of transcription factors and general transcription machinery to the HIV-1 5' LTR. At late time points postinfection, there is decreased NF-κB p65, RNA polymerase II, and p-TEFb bound to the viral promoter (Figure 3). These changes are a consequence of type I IFN signaling in MDMs, as blocking type I IFN signaling prevents the dissociation of NF-κB and RNA polymerase II from the viral promoter. The mechanism of type I IFN-mediated suppression of NF-κB activ-

ity in the context of HIV-1 infection is unknown. Possible mechanisms include synthesis of I $\kappa$ B proteins, increased IRAK-M activity, increased activity of the A20 deubiquitinase, decreased production, sequestration, or increased degradation of NF- $\kappa$ B subunits, or obstruction of the NF- $\kappa$ B binding sites within the HIV-1 5' LTR. These mechanisms will be explored in future studies.

The ability of HIV-1 infection to induce an IFN response has been a subject of controversy, with some reports indicating that HIV-1 induces a potent IFN response<sup>35</sup> and others suggesting that it does not.<sup>51</sup> We recently demonstrated that HIV-1 infection induces a muted IFN response in MDMs.<sup>18</sup> Here, we demonstrate that type I IFN signaling contributes to the establishment of HIV-1 latency in MDMs. Three lines of evidence support this conclusion: (1) treatment of infected MDMs with exogenous type I IFNs leads to a pronounced and sustained decrease in viral replication; (2) blocking IFN signaling in response to endogenous IFNs prevents the establishment of viral latency; and (3) blocking IFN signaling prevents the dissociation of NF- $\kappa$ B and RNA polymerase II from the promoter and maintains the chromatin associated with the transcription start site in an inaccessible state (Figure 4). Although the IFN response is muted,<sup>18</sup> HIV-1 infection does lead to the differential expression of a number of known IRGs, including IFN- $\beta$ , IFI16, IFITM1, MX1, and OASL, among others. Furthermore, when comparing HIV-1 infected MDMs with high levels of viral transcripts to those with low levels of viral transcripts, IRGs are greatly enriched among DEGs. It will be interesting to determine which IRGs are important for the establishment and maintenance of latency in macrophages. A number of IRGs have been shown to inhibit HIV-1 infection at different steps of the viral life cycle, including transcription where IFI16 targets the transcription factor Sp1 to suppress HIV-1 transcription.<sup>52</sup>

HIV-1 can be sensed by a number of different innate immune receptors, including cGAS and RIG-I/MDA5 which signal through STING and MAVS, respectively, to produce an IFN response.<sup>43,53-55</sup> We show that signaling through MAVS is required for the establishment of latent infection in MDMs (Figure 5). A role for MAVS-induced type I IFN secretion in the repression of HIV-1 replication has been shown in T cells.<sup>56</sup> It is possible that newly synthesized intron containing viral RNAs are recognized by MAVS and an as yet undefined RNA sensor, leading to the production of type I IFNs, as has been described for macrophages, dendritic cells, and microglia.<sup>57-59</sup> Alternatively, endogenous ligands for RIG-I or MDA5, such as endogenous retroviral RNAs<sup>60</sup> or short interspersed elements,<sup>61</sup> may also contribute to type I IFN production in HIV-1-infected macrophages. Further exploration of the possible mechanisms leading to type I IFN production, and their contribution to the establishment of viral latency in infected macrophages, is warranted.

Finally, we demonstrate that the HIV-1 accessory protein, Vpr contributes to the induction of viral latency in macrophages through an as yet undefined mechanism (Figure 6). Neither the G2/M cell cycle arrest function nor the DCAF binding function of Vpr is required for this effect. Interestingly, Vpr has been shown to induce a number of IRGs with putative antiviral functions, including RIG-I.<sup>62</sup> RIG-I is a cytosolic RNA sensor upstream of MAVS, a signal transduction protein that we demonstrate is essential for establishing latent infection in MDMs. Our

single cell RNA sequencing data demonstrated that, although RIG-I was up-regulated in HIV-1 infected cells, it was not differentially expressed in cells transitioning to latent infection. It will be important to determine the mechanism through which Vpr contributes to the establishment of latent HIV-1 infection in MDMs and whether it involves up-regulation of RIG-I or another component in the RIG-I/MDA5/MAVS signaling pathway.

## ACKNOWLEDGMENTS

This work was supported by a University of Utah School of Medicine Research Initiative Seed Grant (T.H.), the Department of Pathology, University of Utah School of Medicine (T. H.), and the National Institutes of Health ([www.nih.gov](http://www.nih.gov)) grant AI143567-02 (V. P.).

## AUTHORSHIP

*Conceptualization:* V. P. and T. H. *Investigation:* L. D., L. M., and T. H. *Data acquisition and curation:* L. D. and T. H. *Writing (original draft):* L. D. and T. H. *Writing (review, editing, and revision):* L. D., L. M., V. P., and T. H.

## DISCLOSURE

The authors declare no conflict of interest

## REFERENCES

- Gallant J, Hsue PY, Shrey S, Meyer N. Comorbidities among US patients with prevalent HIV INFECTION-A trend analysis. *J Infect Dis.* 2017;216:1525-1533.
- Finzi D, Hermankova M, Pierson T, et al. Identification of a reservoir for HIV-1 in patients on highly active antiretroviral therapy. *Science.* 1997;278:1295-300.
- Chun TW, Carruth L, Finzi D, et al. Quantification of latent tissue reservoirs and total body viral load in HIV-1 infection. *Nature.* 1997;387:183-8.
- Wong JK, Hezareh M, Gunthard HF, et al. Recovery of replication-competent HIV despite prolonged suppression of plasma viremia. *Science.* 1997;278:1291-5.
- Bosque A, Planelles V. Induction of HIV-1 latency and reactivation in primary memory CD4+ T cells. *Blood.* 2009;113:58-65.
- Martins LJ, Bonczkowski P, Spivak AM, et al. Modeling HIV-1 latency in primary T cells using a replication-competent virus. *AIDS Res Hum Retroviruses.* 2016;32:187-93.
- Wong ME, Jaworowski A, Hearps AC. The HIV reservoir in monocytes and macrophages. *Front Immunol.* 2019;10:1435.
- Wiley CA, Schrier RD, Nelson JA, Lampert PW, Oldstone MB. Cellular localization of human immunodeficiency virus infection within the brains of acquired immune deficiency syndrome patients. *Proc Natl Acad Sci USA.* 1986;83:7089-93.
- Gavegnano C, Schinazi RF. Antiretroviral therapy in macrophages: implication for HIV eradication. *Antivir Chem Chemother.* 2009;20:63-78.
- Ganor Y, Real F, Sennepin A, et al. HIV-1 reservoirs in urethral macrophages of patients under suppressive antiretroviral therapy. *Nat Microbiol.* 2019;4:633-644.
- Graziano F, Aimola G, Forlani G, et al. Reversible human immunodeficiency virus Type-1 latency in primary human monocyte-derived macrophages induced by sustained M1 polarization. *Sci Rep.* 2018;8:14249.
- Honeycutt JB, Thayer WO, Baker CE, et al. HIV persistence in tissue macrophages of humanized myeloid-only mice during antiretroviral therapy. *Nat Med.* 2017;23:638-643.

13. Abreu C, Shirk EN, Queen SE, et al. Brain macrophages harbor latent, infectious simian immunodeficiency virus. *Aids*. 2019;33:S181-s188.
14. Abreu CM, Veenhuis RT, Avalos CR, et al. Infectious virus persists in CD4(+) T cells and macrophages in antiretroviral therapy-suppressed simian immunodeficiency virus-infected macaques. *J Virol*. 2019;93:e00065-19.
15. Viglianti GA, Planelles V, Hanley TM. Interactions with commensal and pathogenic bacteria induce HIV-1 latency in macrophages through altered transcription factor recruitment to the LTR. *J Virol*. 2021.
16. Wong ME, Johnson CJ, Hearps AC, Jaworowski A. Development of a novel in vitro primary human monocyte-derived macrophage model to study reactivation of HIV-1 transcription. *J Virol*. 2021;95:e0022721.
17. Szaniawski MA, Spivak AM, Cox JE, et al. SAMHD1 phosphorylation coordinates the anti-HIV-1 response by diverse interferons and tyrosine kinase inhibition. *mBio*. 2018;9:e00819-18.
18. Martins LJSMA, Williams ESCP, Coiras M, Hanley TM, Planelles V. HIV-1 accessory proteins impart a modest interferon response and upregulate cell cycle-related genes in macrophages. *Pathogens*. 2022;11:163.
19. Hanley TM, Viglianti GA. Nuclear receptor signaling inhibits HIV-1 replication in macrophages through multiple trans-repression mechanisms. *J Virol*. 2011;85:10834-50.
20. Cribbs SK, Lennox J, Caliendo AM, Brown LA, Guidot DM. Healthy HIV-1-infected individuals on highly active antiretroviral therapy harbor HIV-1 in their alveolar macrophages. *AIDS Res Hum Retroviruses*. 2015;31:64-70.
21. DiNapoli SR, Ortiz AM, Wu F, et al. Tissue-resident macrophages can contain replication-competent virus in antiretroviral-naive, SIV-infected Asian macaques. *JCI Insight*. 2017;2:e91214.
22. Josefsson L, von Stockenström S, Faria NR, et al. The HIV-1 reservoir in eight patients on long-term suppressive antiretroviral therapy is stable with few genetic changes over time. *Proc Natl Acad Sci USA*. 2013;110:E4987-96.
23. Ko A, Kang G, Hattler JB, et al. Macrophages but not astrocytes harbor HIV DNA in the brains of HIV-1-infected aviremic individuals on suppressive antiretroviral therapy. *J Neuroimmune Pharmacol*. 2019;14:110-119.
24. Yukl SA, Sinclair E, Somsouk M, et al. A comparison of methods for measuring rectal HIV levels suggests that HIV DNA resides in cells other than CD4+ T cells, including myeloid cells. *AIDS*. 2014;28:439-42.
25. Zalar A, Figueroa MI, Ruibal-Ares B, et al. Macrophage HIV-1 infection in duodenal tissue of patients on long term HAART. *Antiviral Res*. 2010;87:269-71.
26. Szaniawski MA, Spivak AM, Bosque A, Planelles V. Sex influences SAMHD1 activity and susceptibility to human immunodeficiency virus-1 in primary human macrophages. *J Infect Dis*. 2019;219:777-785.
27. Laguette N, Sobhian B, Casartelli N, et al. SAMHD1 is the dendritic and myeloid-cell-specific HIV-1 restriction factor counteracted by Vpx. *Nature*. 2011;474:654-7.
28. Van Lint C, Emiliani S, Ott M, Verdin E. Transcriptional activation and chromatin remodeling of the HIV-1 promoter in response to histone acetylation. *EMBO J*. 1996;15:1112-20.
29. Verdin E, Paras P, Van Lint C. Chromatin disruption in the promoter of human immunodeficiency virus type 1 during transcriptional activation. *EMBO J*. 1993;12:3249-59.
30. El Kharroubi A, Piras G, Zensen R, Martin MA. Transcriptional activation of the integrated chromatin-associated human immunodeficiency virus type 1 promoter. *Mol Cell Biol*. 1998;18:2535-44.
31. Yukl SA, Kaiser P, Kim P, et al. HIV latency in isolated patient CD4(+) T cells may be due to blocks in HIV transcriptional elongation, completion, and splicing. *Sci Transl Med*. 2018;10:eaap9927.
32. Budhiraja S, Famiglietti M, Bosque A, Planelles V, Rice AP. Cyclin T1 and CDK9 T-loop phosphorylation are downregulated during establishment of HIV-1 latency in primary resting memory CD4+ T cells. *J Virol*. 2013;87:1211-20.
33. Tyagi M, Pearson RJ, Karn J. Establishment of HIV latency in primary CD4+ cells is due to epigenetic transcriptional silencing and P-TEFb restriction. *J Virol*. 2010;84:6425-37.
34. Altfeld M. Innate immunity against HIV-1 infection. *Nat Immunol*. 2015;16:554-62.
35. Decalf J, Desdouits M, Rodrigues V, et al. Sensing of HIV-1 entry triggers a type I interferon response in human primary macrophages. *J Virol*. 2017;91:e00147-17.
36. Berger G, Durand S, Fargier G, et al. APOBEC3A is a specific inhibitor of the early phases of HIV-1 infection in myeloid cells. *PLoS Pathog*. 2011;7:e1002221.
37. Kane M, Zang TM, Rihn SJ, et al. Identification of interferon-stimulated genes with antiretroviral activity. *Cell Host Microbe*. 2016;20:392-405.
38. Ullah H, Sajid M, Yan K, et al. Antiviral activity of interferon alpha-inducible protein 27 against hepatitis B virus gene expression and replication. *Front Microbiol*. 2021;12:656353.
39. Breckpot K, Escors D, Arce F, et al. HIV-1 lentiviral vector immunogenicity is mediated by Toll-like receptor 3 (TLR3) and TLR7. *J Virol*. 2010;84:5627-36.
40. Heil F, Hemmi H, Hochrein H, et al. Species-specific recognition of single-stranded RNA via toll-like receptor 7 and 8. *Science*. 2004;303:1526-9.
41. Beignon AS, McKenna K, Skoberne M, et al. Endocytosis of HIV-1 activates plasmacytoid dendritic cells via Toll-like receptor-viral RNA interactions. *J Clin Invest*. 2005;115:3265-75.
42. Gringhuis SI, van der Vlist M, van den Berg LM, den Dunnen J, Litjens M, Geijtenbeek TB. HIV-1 exploits innate signaling by TLR8 and DC-SIGN for productive infection of dendritic cells. *Nat Immunol*. 2010;11:419-26.
43. Berg RK, Melchjorsen J, Rintahaka J, et al. Genomic HIV RNA induces innate immune responses through RIG-I-dependent sensing of secondary-structured RNA. *PLoS One*. 2012;7:e29291.
44. Gao D, Wu J, Wu YT, et al. Cyclic GMP-AMP synthase is an innate immune sensor of HIV and other retroviruses. *Science*. 2013;341:903-6.
45. Maitra RK, McMillan NA, Desai S, et al. HIV-1 TAR RNA has an intrinsic ability to activate interferon-inducible enzymes. *Virology*. 1994;204:823-7.
46. DeHart JL, Zimmerman ES, Ardon O, Monteiro-Filho CM, Arganaraz ER, Planelles V. HIV-1 Vpr activates the G2 checkpoint through manipulation of the ubiquitin proteasome system. *Virology*. 2007;4:57.
47. Ancuta P, Kunstman KJ, Autissier P, et al. CD16+ monocytes exposed to HIV promote highly efficient viral replication upon differentiation into macrophages and interaction with T cells. *Virology*. 2006;344:267-76.
48. Ellery PJ, Tippett E, Chiu YL, et al. The CD16+ monocyte subset is more permissive to infection and preferentially harbors HIV-1 in vivo. *J Immunol*. 2007;178:6581-9.
49. Jaworowski A, Kamwendo DD, Ellery P, et al. CD16+ monocyte subset preferentially harbors HIV-1 and is expanded in pregnant Malawian women with Plasmodium falciparum malaria and HIV-1 infection. *J Infect Dis*. 2007;196:38-42.
50. Moniuszko M, Liyanage NP, Doster MN, et al. Glucocorticoid treatment at moderate doses of SIVmac251-infected rhesus macaques decreases the frequency of circulating CD14+CD16++ monocytes but does not alter the tissue virus reservoir. *AIDS Res Hum Retroviruses*. 2015;31:115-26.
51. Cingoz O, Goff SP. HIV-1 is a poor inducer of innate immune responses. *MBio*. 2019;10:e02834-18.
52. Hotter D, Bosso M, Jonsson KL, et al. IFI16 targets the transcription factor Sp1 to suppress HIV-1 transcription and latency reactivation. *Cell Host Microbe*. 2019;25:858-872.e13.

53. Sumner RP, Harrison L, Touizer E, et al. Disrupting HIV-1 capsid formation causes cGAS sensing of viral DNA. *EMBO J.* 2020;39:e103958.
54. Wang MQ, Huang YL, Huang J, Zheng JL, Qian GX. RIG-I detects HIV-1 infection and mediates type I interferon response in human macrophages from patients with HIV-1-associated neurocognitive disorders. *Genet Mol Res.* 2015;14:13799-811.
55. Nasr N, Alshehri AA, Wright TK, et al. Mechanism of interferon-stimulated gene induction in HIV-1-infected macrophages. *J Virol.* 2017;91:e00744-17.
56. Gupta S, Termini JM, Issac B, Guirado E, Stone GW. Constitutively active MAVS inhibits HIV-1 replication via type I interferon secretion and induction of HIV-1 restriction factors. *PLoS One.* 2016;11:e0148929.
57. Akiyama H, Jalloh S, Park S, Lei M, Mostoslavsky G, Gummuluru S. Expression of HIV-1 intron-containing RNA in microglia induces inflammatory responses. *J Virol.* 2020;95.
58. Akiyama H, Miller CM, Ettinger CR, Belkina AC, Snyder-Cappione JE, Gummuluru S. HIV-1 intron-containing RNA expression induces innate immune activation and T cell dysfunction. *Nat Commun.* 2018;9:3450.
59. McCauley SM, Kim K, Nowosielska A, et al. Intron-containing RNA from the HIV-1 provirus activates type I interferon and inflammatory cytokines. *Nat Commun.* 2018;9:5305.
60. Zeng M, Hu Z, Shi X, et al. MAVS, cGAS, and endogenous retroviruses in T-independent B cell responses. *Science.* 2014;346:1486-92.
61. Leonova KI, Brodsky L, Lipchick B, et al. p53 cooperates with DNA methylation and a suicidal interferon response to maintain epigenetic silencing of repeats and noncoding RNAs. *Proc Natl Acad Sci USA.* 2013;110:E89-98.
62. Zahoor MA, Xue G, Sato H, Murakami T, Takeshima SN, Aida Y. HIV-1 Vpr induces interferon-stimulated genes in human monocyte-derived macrophages. *PLoS One.* 2014;9:e106418.
63. Williams SA, Chen LF, Kwon H, Ruiz-Jarabo CM, Verdin E, Greene WC. NF-kappaB p50 promotes HIV latency through HDAC recruitment and repression of transcriptional initiation. *EMBO J.* 2006;25:139-49.

## SUPPORTING INFORMATION

Additional supporting information can be found online in the Supporting Information section at the end of this article.

**How to cite this article:** Dickey LL, Martins LJ, Planelles V, et al. HIV-1-induced type I IFNs promote viral latency in macrophages. *J Leukoc Biol.* 2022;112:1343–1356.  
<https://doi.org/10.1002/JLB.4MA0422-616R>